Scientific Research Publishing

Open Journal of Civil Engineering, 2025, 15(2), 182-204
https://www.scirp.org/journal/ojce
ISSN Online: 2164-3172
ISSN Print: 2164-3164

Mechanical Performance of Ultra-High Performance Concrete Reinforced with Micro Steel Fibers: Experimental and Numerical Investigation under Uniaxial Compression and Flexural Loading

Yan Li[1*], Gabi Benaiah Jonathan[1], Kambale Kamate Merveille[2]

[1]College of Civil Engineering, Jilin Jianzhu University, Changchun, China
[2]School of Civil Engineering and Architecture, Wuhan University of Technology, Wuhan, China
Email: *lessle@126.com

How to cite this paper: Li, Y., Jonathan, G.B. and Merveille, K.K. (2025) Mechanical Performance of Ultra-High Performance Concrete Reinforced with Micro Steel Fibers: Experimental and Numerical Investigation under Uniaxial Compression and Flexural Loading. *Open Journal of Civil Engineering*, **15**, 182-204.
https://doi.org/10.4236/ojce.2025.152011

Received: April 29, 2025
Accepted: June 21, 2025
Published: June 24, 2025

Abstract

This study investigates the optimal steel fiber volume ratio (0% - 5%) in Ultra-High-Performance Concrete (UHPC) to balance mechanical performance and cost efficiency. Combining experimental testing (up to 3% fibers) and Finite Element Modeling (FEM) in ABAQUS (extended to 5%), the research evaluates two reinforcement systems: 1) monolithic 13 mm micro steel fibers (0.5% - 5%) and 2) a hybrid mix of 13 mm micro and 20 mm recycled steel fibers (2.5% - 3.5%). Results identify 3% - 3.5% as the optimal range, with hybrid fibers improving flexural strength but reducing ductility and stiffness compared to mono-fiber UHPC. FEM simulations closely matched experiments, validating computational modelling for UHPFRC analysis. The findings provide practical guidance for mix design, address gaps in standards (e.g., ACI 544.1R), and highlight the need for further research on hybrid fiber optimization. This work supports UHPFRC adoption in high-demand applications like seismic-resistant infrastructure and long-span bridges, advancing sustainable, high-performance construction.

Keywords

Mechanical Properties, Ultra-high Performance Fiber Reinforced Concrete (UHPFRC), Micro Steel Fibers, Fiber Volume Ratio

1. Introduction

Concrete is the cornerstone of modern construction, prized for its durability, ver-

satility, and cost-efficiency [1]-[4]. Among its advanced variants, Ultra-High-Performance Concrete (UHPC) has gained prominence due to its superior mechanical properties and enhanced resilience against multi-hazard conditions [5]-[8]. The performance of UHPC is critically influenced by steel fiber characteristics—including geometry, volume fraction, and alignment—which govern its tensile strength, crack resistance, and ductility [3] [8]-[13]. Fiber orientation and length significantly influence performance, as aligned 20 mm fibers demonstrate superior mechanical behavior compared to shorter, randomly distributed fibers at equal dosages [14] [15]. Perpendicular fiber alignment enhances tensile strength and fracture energy by 21% and 47%, respectively [16], underscoring the need for controlled distribution [17] [18]. While hybrid systems (e.g., micro and recycled steel fibers) improve sustainability, ductility trade-offs necessitate further optimization However, despite extensive research, the optimal fiber content remains contentious, with studies reporting conflicting results on strength improvements beyond 1% - 5% fiber volume (Vf) [19]-[21]. While UHPC demonstrates exceptional thermal and impact resistance [22]-[24], existing studies have yet to systematically optimize fiber volume ratio (Vf) to balance structural performance and economic viability. This study addresses this gap by investigating the effects of steel fiber volume ratio (Vf) content (0.5% - 5%) on UHPC's mechanical behaviour through experimental testing and numerical simulations (ABAQUS), to establish practical guidelines for resilient infrastructure design.

The increasing demand for sustainable, high-performance materials has further highlighted the potential of Ultra-High-Performance Fiber-Reinforced Concrete (UHPFRC). Despite its advantages, critical knowledge gaps persist regarding steel-fiber-reinforced UHPFRC, particularly in understanding its behavior under varied loading conditions and identifying the optimal fiber volume ratio that maximizes structural efficiency without compromising cost-effectiveness. Current design practices often lack empirical guidance, resulting in either over-engineering or premature failure. Furthermore, key failure mechanisms—such as stiffness degradation, post-peak behavior, and crack propagation—remain inadequately characterized, limiting the accuracy of predictive models.

This study aims to bridge these gaps by 1) experimentally evaluating the influence of steel fiber volume ratio (Vf) (at a constant aspect ratio) on uniaxial compressive and four-point flexural strength, 2) validating findings through ABAQUS finite element simulations, and 3) analyzing failure modes to develop practical mix design guidelines. The research objectives include quantifying mechanical performance relative to fiber content, assessing crack-arresting mechanisms and ductility, determining the optimal fiber ratio for cost-effective high performance, and improving the reliability of computational modelling. By integrating theoretical and empirical insights, this work advances the application of UHPFRC in resilient and sustainable infrastructure, offering validated design strategies that minimize material waste, extend service life, and reduce environmental impact—addressing a pressing need in contemporary civil engineering.

2. Experimental Preparations

2.1. Materials and Specimen Preparation

To investigate the influence of steel fiber in ultra-high performance concrete mix that was cured at natural environmental conditions in five specimen groups categorized by differences in fiber volume ratio (Vf) from the initial specimen group of 1% fiber volume ratio up to the last specimen group of 3% with 0.5% volume rate increment for steel fibers from the first up to the last specimen group. Conducting laboratory UHPC with steel fiber volume ratio (Vf) beyond 3% experimental evaluations poses a challenge on controlling the flowability of fresh concrete [25] because steel fibers significantly reduces fluidity of fresh concrete [26].

The primary ingredients were special reactive powder concrete, steel fiber, and water. Special reactive powder concrete is a new construction engineering material used to make UHPC in China. It is special because all necessary fine aggregates, including silica fume, binders, and other reactive admixtures, are already mixed during manufacturing, making it easy for application in the construction industry since primary aggregates are already mixed at respective optimum ratios. UHPC copper-coated micro steel fiber was mixed in the five specimen groups at different fiber volume percentages of 1%, 1.5%, 2%, 2.5%, and 3%, respectively. Table 1 illustrates the characteristics of steel fiber specified according to manufacturer's standards, and Figure 1 shows the materials used in the mix design. The water-to-cement ratio w/c was 0.2 which is according to the design mix of UHPC standards.

Figure 1. Materials used in the design mix: (a) ready-mixed UHPC reactive concrete powder, (b) 13 mm length UHPC steel fiber, and (c) measured steel fiber.

Table 1. Characteristics of steel fiber.

Steel fiber type	Length (mm)	Diameter (mm)	Fiber aspect ratio (l/d)	Tensile Yield strength (MPa)
UHPC copper-coated micro steel fiber	13	0.2	65	2850

Casting design mix

At first, a UHPC horizontal mix rotating drum was used to mix the three components. The UHPC horizontal mix rotating drum's main advantage is that it

evenly distributes micro steel fibers along the horizontal length, positively influencing fiber orientation during mixing as an agglomeration of fiber will be avoided. The long, curved blades make it more convenient to evenly spread the steel fiber within the drum, as shown in Figure 2. I firstly poured reactive powder concrete into the drum and rotated it for about a minute then slowly added water periodically after every forty-five seconds rotation to make sure the powder was evenly mixed with water until all the w/c of 0.2 was fully mixed then later carefully added the steel fiber according to respective specimen volume ratios in small portions each moment until all the steel fiber was fully blended. Each load took about six and a half minutes to fully mix until ready to be cast into respective molds for curing.

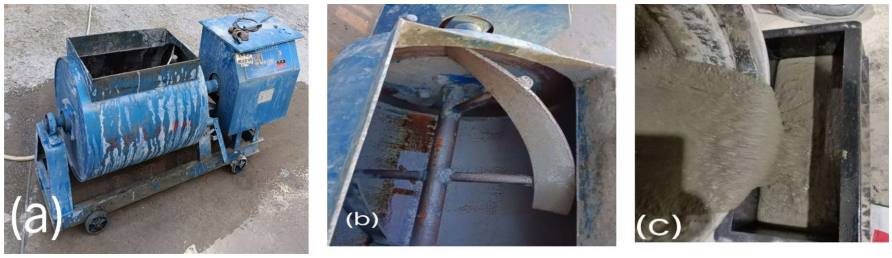

Figure 2. UHPC horizontal mix rotating drum (a) the exterior, (b) the interior, and (c) ready fresh concrete.

Test specimens in this experimental program were cured in natural environmental conditions in open weather. October (end of spring) in Changchun, China, ranges from an average temperature of 5 degrees Celsius in the early morning to 22 degrees Celsius in the afternoon. The cast specimens were de-molded after 7 days of casting, then later put in an laboratory store room and were regularly water sprayed at room temperature water on the surface until 28 days of curing were complete, as shown in Figure 3, then tested for uniaxial compressive strength and flexural strength under four-point beam load conditions at a later stage.

Figure 3. (a) fresh concrete cast specimen (b) spayed concrete specimens after demolding under 28 days curing process.

Hybrid Fiber Study

This section examines the mechanical performance of concrete prism specimens reinforced with a hybrid mix of 13 mm micro-steel fibers and 20 mm recycled steel fibers (1:1 ratio) at 2.5%, 3%, and 3.5% volume fractions which portrayed best flexural performance in previous tests. Numerical simulations assess their be-

havior under four-point bending test. Increasing length of steel fibers has no significant improvement towards compressive strength of UHPC [27] [28] but long steel fibers exhibit higher flexural strength than short fibers [29] therefore this part only focused on flexural test evaluations. Previous tests using only micro-steel fibers showed superior results but high cost, whereas recycled fibers offer a cost-effective alternative (10 times cheaper) [30]. The hybrid approach balances performance and affordability in (UHPC). Key fiber parameters are provided in Table 2.

Table 2. Parameters for steel fiber.

Material	Length (mm)	Diameter (mm)	Fiber Aspect Ratio (Vf)	Fiber Density	Young Modulus	Poison Ratio
UHPC copper-coated micro-steel fiber	13	0.2	65	7.8E−09	210,000	0.3
Industrially recycled fiber	20	0.4	50	7.8E−09	199,000	0.3

2.2. Experimental Testing

After 28 days of curing, both compressive and flexural tests were conducted. 100mm cubes were tested for compression, while the 1000 mm × 100 mm × 300 mm prism specimens for all five groups were tested for flexure at Jilin Jianzhu University engineering simulation and research laboratory (as illustrated in Figure 4). YAR 2000 is the type of hydraulic jack that can administer loads up to 2000 KN, and it was used to perform both tests for all five specimen groups.

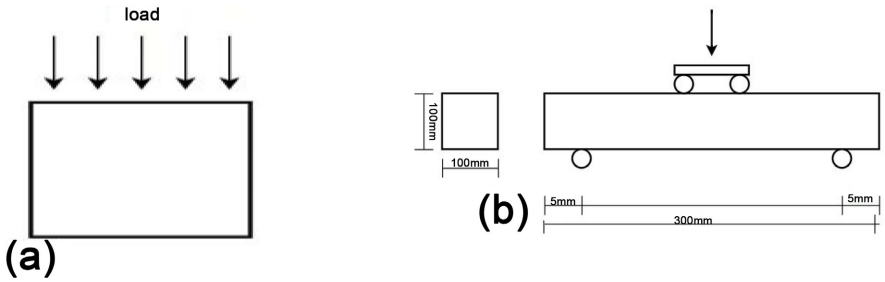

Figure 4. (a) Shows the direction load of the cube under compression test; (b) shows the flexural setup prisms.

Firstly, the compressive load was applied at a rate of 1 MPa/s and gave excellent results, but after realizing that the rate was too fast as the test was performed in under a minute, the compressive load rate was later reduced to 0.5 MPa/s for the rest of the compressive tests. The flexural strength was loaded at a rate of 0.1 MPa/s. The beam was subjected to two equally concentrated loads at 50 mm from the mid-span via a four-point loading method. A single hydraulically actuated jack was used to supply the monotonically increasing load through a displacement control method. Figure 5 shows the actual test setup for (a) the compression test and (b) the four-point loading test, which was the actual setup for all specimens tested.

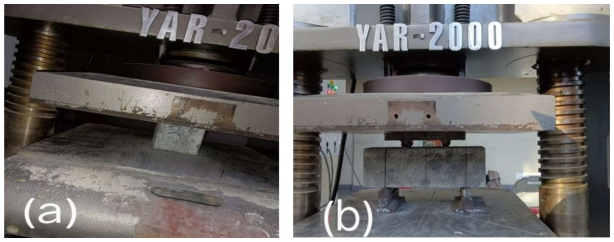

Figure 5. Experimental test set up for (a) compression test (b) four-point flexural test.

2.3. Numerical Modeling (ABAQUS)

This study used Finite Element Analysis (FEA) in ABAQUS to analyze steel fiber-reinforced ultra-high-performance concrete under uniaxial compression and four-point bending. The Concrete Damaged Plasticity model simulated concrete's nonlinear behavior, with material properties derived from lab tests (Young's Modulus: 39,100 MPa, Poisson's ratio: 0.2). Python scripting automated modeling, while steel fibers were represented as line elements. Nine specimen groups with steel fiber volumes ranging from 1% to 5% (in 0.5% increments) were tested. For compression, 100 mm cubes were used, and 100 × 100 × 300 mm prisms were tested in bending. A 1 MPa load rate was applied along the y-axis, with the bottom surface fully constrained. Frictional contact (μ = 0.3) was set for bending tests. Specimen loading configurations are illustrated in **Figure 6**.

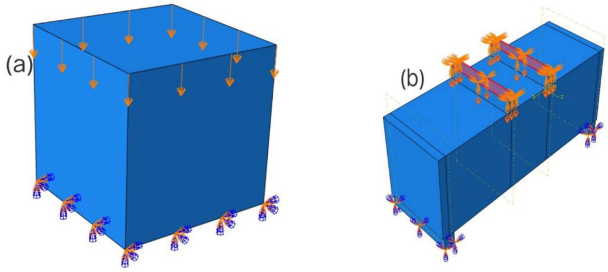

Figure 6. Loaded sample specimens for (a) concrete cube and (b) prism specimen.

Both specimen samples were globally meshed within the meshing range parameters prescribed in the simulation software. When dividing the mesh of the specimen model, the size of the mesh defines the degree of accuracy of the results and the period for analysis; therefore, observing the density of mesh divisions is essential in the finite element analysis process. Adopting a reasonable mesh size division [31] [32] improves the convergence of simulation results. **Figure 7** shows meshed samples of (a) a concrete cube and (b) a prism specimen with a global mesh size of 10.

2.4. Data Calculation Model

Resistance forces of sections subjected to flexure are calculated from a linear strain

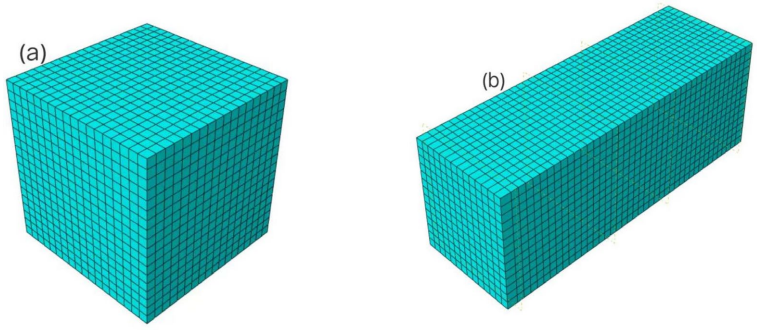

Figure 7. Meshed (a) concrete cube and (b) concrete prism.

diagram that is bounded by compression strain limit corresponding to UHPC crushing and reinforcing steel limits that correspond to rupture of reinforcing steel, but members that do not have steel reinforcing bars or pre-stressed strands, the strains are limited to strain at peak tensile strength of UHPC [33]. UHPC is a material that is still being researched. Hence, there is a lack of abundant data that can be referred to come up with a factor of factored flexural resistance, but the LRFD guidelines that propose flexural resistance M_r = resistance factor for flexural moment $\varnothing_f$ multiplied by nominal flexure moment M_n. The resistance factor $\varnothing_f$ calculations are well elaborated in AASHTO LRFD BDS [34].

The ductility factors of a structure are the maximum deformation or ultimate load divided by the corresponding deformation or load at yield. It is a useful non-dimensional index of inelastic deformation. $\mu = \theta$ ultimate/θ yield where μ is ductility index, θ ultimate is max load or deformation, and θ yield is yield load or deformation [35]. The ductility of concrete beams can be quantified using the ductility index expressed by the deflection ductility index, curvature ductility index, or rotational ductility index. After a flexural test on a concrete beam, mid-span deflection can be used to get the ductility index where the above equation will be adjusted to ɵ ultimate being mid-span deflection at ultimate load and ɵ yield as mid-span deflection at yield load [36]. This paper used the deflection ductility index to calculate ductility. The curvature ductility ratio uses the bending moment at the ultimate load divided by the bending moment at the yield load. If the curvature ductility ratio > 2.0, the flexural resistance of the member is taken equal to the moment at a yield of reinforcement, but if the curvature ductility ratio < 2.0, then the flexural resistance of the member must be taken as max of 0.5 of the moment or flexural resistance calculated without considering the contribution of steel fibers [38]. Flexural strength was calculated as given by the equation according to GB50081-2019 as follows:

$$f = \frac{Fl}{bh^2} \tag{2-1}$$

In Equation (2-1), F is the load applied at failure, l is the length of the span, b is the width of the specimen, and h is the height of the specimen.

The deflection ductility index was used to calculate the ductility of the beams.

$$\mu = \frac{\Delta u}{\Delta y} \tag{2-2}$$

In Equation (2-2), Δu is the deflection at the ultimate load, while Δy is the deflection at the yield load [36].

In reality, reinforced concrete beams crack (micro-cracks within the specimen) before they even reach the yielding point, which is also known as the point of the first crack. Calculating the service stiffness of a reinforced concrete section according to the load and resistance factors specified in reinforced concrete design codes is essential. Service stiffness is approximately 60% to 70% of the ultimate load [38]. In this experimental setup, 10% before and after the standard gave a more realistic solution; hence, 50% to 80% was considered. Post-peak stiffness is a mechanical behavior of a material after it has reached its ultimate strength and begins to soften or degrade, which quantifies the rate of decline in resistance (stress) with respect to deformation (strain) in the post-peak regime of the stress-strain curve. Calculating post-peak stiffness is also a reliable way to check for the ductility of the beam under a four-point loading test. It is obtained by calculating a slope on the load-deflection curve at points between 90% and 70% of the ultimate load, which is the descending part of the curve just before failure, also regarded as the softening phase.

To analyze the elasticity of a beam under a point loading test other than just relying on the visual analytics of the load-deflection curve, post-elastic strength [39] can be calculated as follows

$$1 - \left[\frac{F(\max) - F(\text{yield})}{F(\text{yield})} \right] \tag{2-3}$$

In Equation (2-3), F(max) is the maximum load (peak state load), and F(yield) is the load at the yield point. The results are a numeration between 0 and 1. Post-elastic strength component 0 is a highly inelastic phase, while 1 is a perfectly elastic phase.

3. Results and Discussion

3.1. Compression Test Results

Table 3. Uniaxial compression load results for laboratory experiments.

Steel fiber reinforcement ratio (%)	Peak state stress (MPa)	0.3 peak state stress (MPa)	0.5 peak state stress (MPa)	Ultimate strain	0.3 peak state strain	0.5 peak state strain	Modulus of elasticity
1%	57.44	17.23	28.27	0.0555	0.01304	0.01571	4269.66
1.5%	65.19	19.56	32.595	0.0616	0.02622	0.02904	4621.765
2.%	62.74	18.82	31.37	0.0953	0.02358	0.02625	4699.625
2.5%	71.40	21.44	35.699	0.0774	0.02319	0.02632	4562.88
3%	84.31	25.29	42.153	0.1435	0.01816	0.02354	3132.639

Table 4. Compression test results for ABAQUS simulation model.

Steel fiber reinforcement ratio (%)	Peak stress (MPa)	0.3 Peak stress (MPa)	0.7 Peak stress (MPa)	Ultimate strain	Strain at 0.3 Peak stress	Strain at 0.7 peak stress	Modulus of elasticity
1%	57.4632	17.2390	40.2242	0.0556	0.00788	0.03055	832.1959
1.5%	60.9601	18.2880	42.6721	0.0591	0.02114	0.0449	1026.6977
2%	68.0362	20.4109	47.6253	0.0552	0.00924	0.03107	1246.6551
2.5%	75.4698	22.64.09	52.8289	0.0409	0.00308	0.0237	1464.0136
3%	84.1797	25.2539	58.9258	0.0584	0.00291	0.00985	4851.8571
3.5%	88.0194	26.4058	61.6136	0.0628	0.00254	0.00598	10243.7504
4%	90.8640	63.6048	63.6048	0.1367	0.00249	0.00857	5975.9290
4.5%	93.0315	65.1220	65.1220	0.1926	0.00278	0.00692	8992.8919
5%	91.675	64.1725	64.1725	0.1851	0.00401	0.00689	12732.639

3.2. Flexural Test Results

Table 5. Four-point loading test results for laboratory experiment.

Concrete specimen groups in terms of their steel fiber reinforcement volume ratio (%)	1	1.5	2	2.5	3
Yield load/load at first crack (KN)	35.7600	50.2400	61.3667	62.0126	78.2816
Ultimate/load at failure (KN)	17.9480	21.5600	28.2200	29.0360	36.8280
Yield deflection (mm)	1.7813	2.5852	2.8071	1.5872	2.2872
Ultimate deflection (mm)	3.5348	3.7220	4.0338	2.9873	3.2784
Ductility index (μ)	1.9844	1.4397	1.4370	1.8821	1.4333
Peak state load (KN)	46.4200	53.9280	72.1960	72.9560	92.096
Peak state deflection (mm)	2.1833	2.8348	2.9941	1.7604	2.4882
Flexural strength (MPa)	5.2049	6.2524	8.1840	8.4200	10.6800
Service stiffness (KN/mm)	15.5753	29.5469	107.7558	143.5369	153.3179
Post-peak stiffness (KN/mm)	3.9639	16.6441	37.1279	203.9500	71.6629
Post elastic strength	0.7019	0.9266	0.8235	0.8111	0.8235

Table 6. Flexural test results for Hybrid fiber study.

Concrete Specimen groups in terms of steel fiber volume ratios (%)	2.5% specimen	3% specimen	3.5% specimen
Load at first crack/yield load (KN)	76.008	84.3830	89.1929
Peak-state Load (KN)	89.4362	99.2742	104.9328
Ultimate/Load at failure (KN)	51.1673	56.9573	42.1489
Yield deflection (mm)	2.4095	2.3197	2.4981
Peak-state deflection(mm)	2.6716	2.5144	2.8346
Ultimate deflection(mm)	4.1388	3.3148	3.6542

Continued

Ductility Index (μ)	1.7175	1.4290	1.4628
Flexural strength (MPa)	14.3268	15.9480	11.8017
Service stiffness (KN/mm)	58.9223	59.3887	29.1342
Post Peak stiffness (KN/mm)	8.1768	26.0098	39.0881

3.3. Discussion

3.3.1. Experimental Trends

Compression test

Ultra-high-performance concrete reinforced with steel fibers relies on the fiber-matrix composite for compressive strength. Ultimate stress increases with the steel fiber volume ratio. Figure 8 shows failure specimens, with 1% fiber content (c) exhibiting larger cracks compared to minimal cracks in (a). Higher fiber ratios (2.5% and 3%) resulted in more ductile failure, reducing disintegration compared to the 1% specimen. Table 3 and Table 4 shows calculated results for compression test results for both laboratory experimental results and numerical simulation model results.

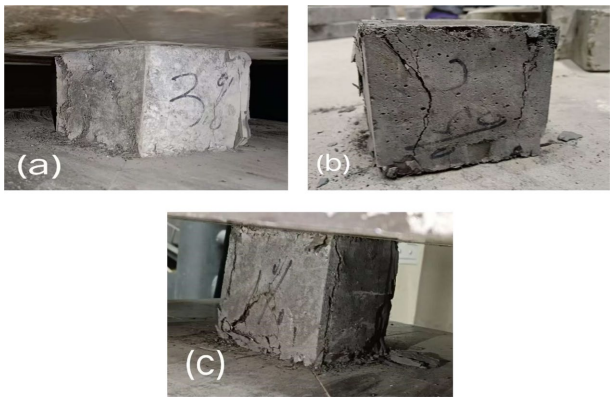

Figure 8. Failure mode after compressive failure for (a) 3%, (b) 2.5%, and (c) 1% steel fiber volume ratio.

Flexural test

The 100 × 100 × 300 mm prism specimens from all five groups underwent flexural testing under a linearly increasing load controlled by a 2000 KN hydraulic actuator. The first crack formation was accompanied by an audible sound, followed by visible micro-cracks at the beam's bottom surface between the loading points. As the load increased, multiple micro-cracks developed until a dominant mid-section crack formed, widening as it propagated upward, absorbing smaller cracks along its path. The 1% steel fiber specimen exhibited two cracks—a primary crack near the left bearing (widest at the bottom) and a minor, narrower crack extending vertically. The 1.5% fiber specimen developed a single crack near the right bearing, extending toward the compression zone, while the 2% fiber specimen showed a similar pattern but with less fiber pull-out. The 2.5% fiber specimen

behaved comparably to the 2% group. In contrast, the 3% fiber specimen displayed a more expansive crack originating near the mid-left, curving upward with minimal fiber pull-out and fewer powdery particles. Figure 9 illustrates the failure patterns for each specimen group (a-f). Calculated four point loading evaluations are well outlined in Table 5.

3.3.2. Numerical Simulation Trends

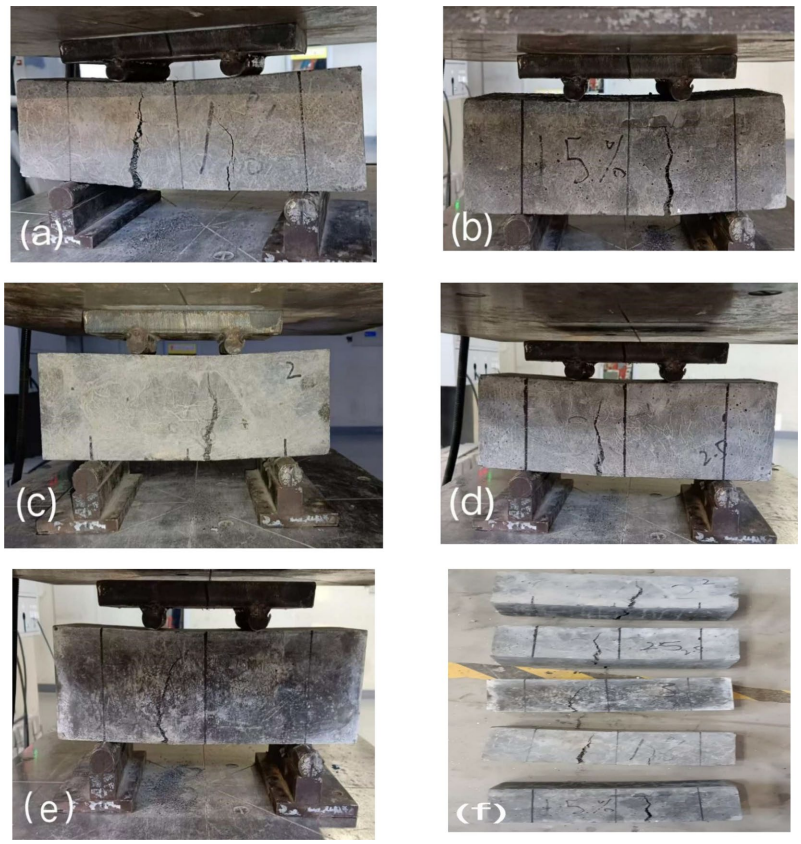

Figure 9. 100 × 100 × 300 mm prism specimens under flexural test for (a) 1%, (b) 1.5%, (c) 2%, (d) 2.5%, (e) 3%, and (f) all five specimen samples after test.

The concrete specimens exhibited varying responses to Von Mises stress, visualized through a color spectrum: red indicated high-stress vulnerability, amber/yellow moderate susceptibility, and green/blue zones with minimal deformation. Specimens with lower steel fiber ratios (e.g., 1%) showed limited stress resistance, evidenced by dominant blue surfaces (Figure 10). Higher fiber ratios (1.5% - 2.5%) displayed gradual improvements, with lighter blue tops indicating marginally better absorption. Notably, ratios of 3% - 3.5% demonstrated visibly enhanced stress absorption, while 4% - 5% ratios achieved peak performance, though no significant gain occurred beyond 4% (constant spectra). Such delicate observation corresponds well with other laboratory experimental evaluations where the compressive strength was 5.06% and 7.6% lower than that of 3% volume fiber at 4% and 5% volume fiber [4]. Another laboratory experimental study revealed that

adding steel fibers from 3% to 45% resulted in reduction of compressive strength from 207 MPa to 158 MPa [40] meaning that fiber volume ratio beyond 3.5% had no significant influence on the compressive strength. Steel fibers predominantly absorbed stresses, exhibiting red spectra at peak failure, confirming their role in transferring internal stresses and boosting compressive strength. This underscores steel fibers' critical contribution to UHPC's stress-resistant capacity.

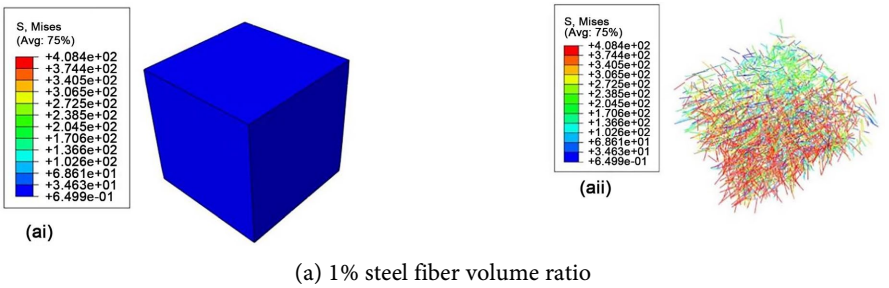

(a) 1% steel fiber volume ratio

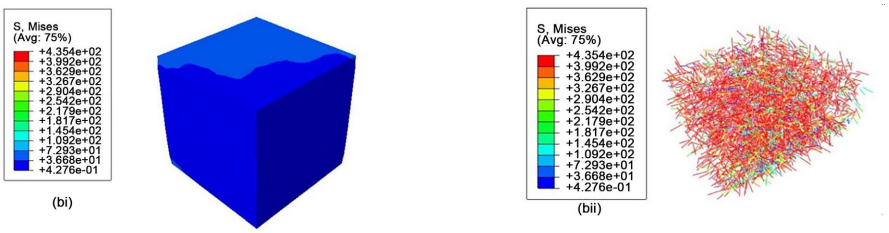

(b) 1.5% steel fiber volume ratio

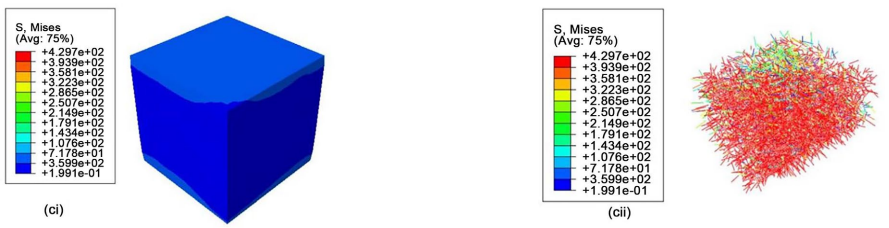

(c) 2% steel fiber volume ratio

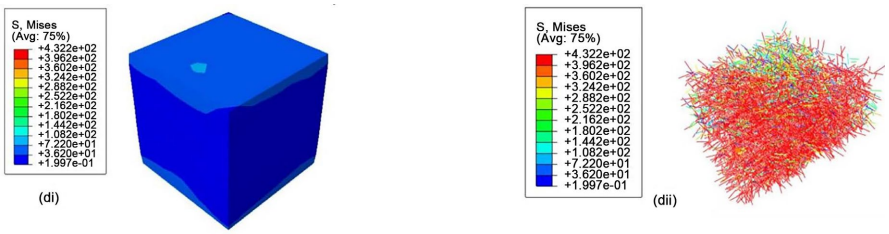

(d) 2.5% steel fiber volume ratio

(e) 3% steel fiber volume ratio

(f) 3.5% steel fiber volume ratio

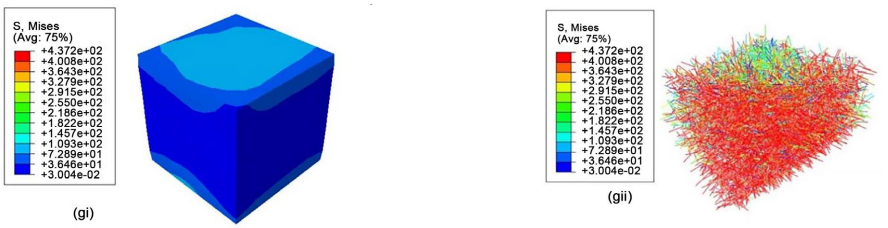

(g) 4% steel fiber volume ratio

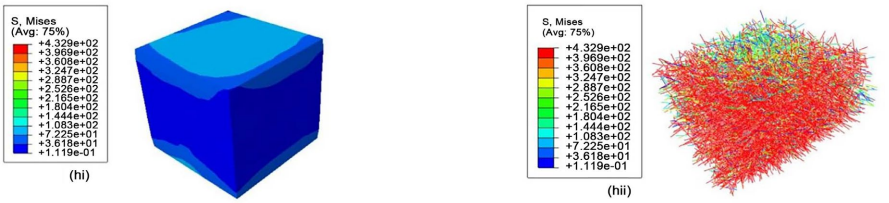

(h) 4.5% steel fiber volume ratio

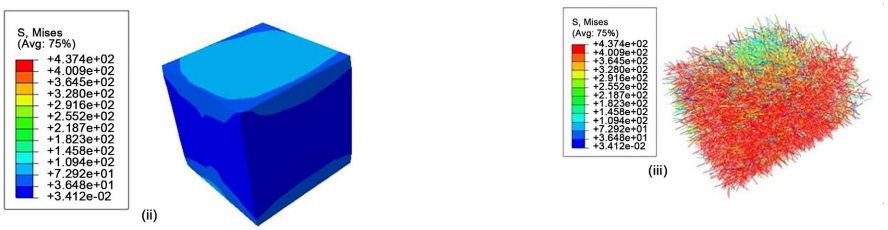

(i) 5% steel fiber volume ratio

Figure 10. Concrete cube specimens after simulation test 1) cube's exterior surface and 2) steel fibers.

Flexural strength test (*Four-point bending load*)

Steel fibers increase concrete beams' flexural resistance under bending. **Figures 11(a)-(j)** shows prisms after testing, with stress absorption rising with fiber content (1% - 5%). More fibers led to higher load-bearing capacity, proving their effectiveness in enhancing flexural performance.

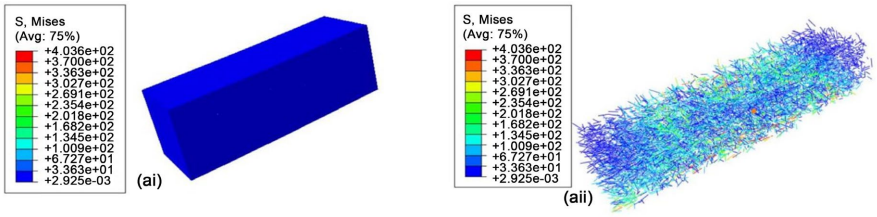

(a) 1% steel fiber volume ratio

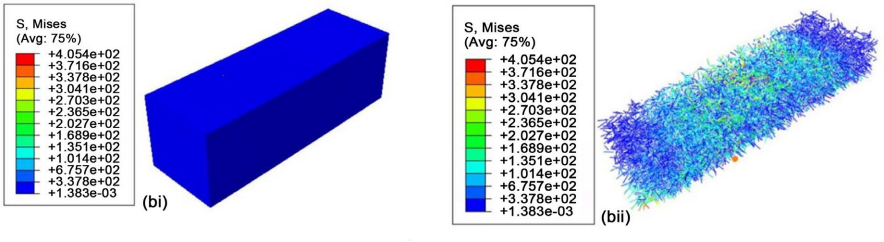

(b) 1.5% steel fiber volume ratio

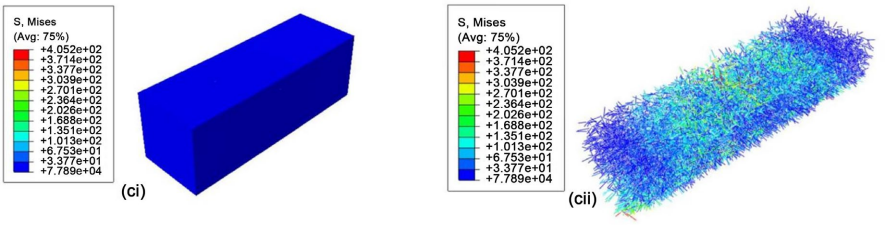

(c) 2% steel fiber volume ratio

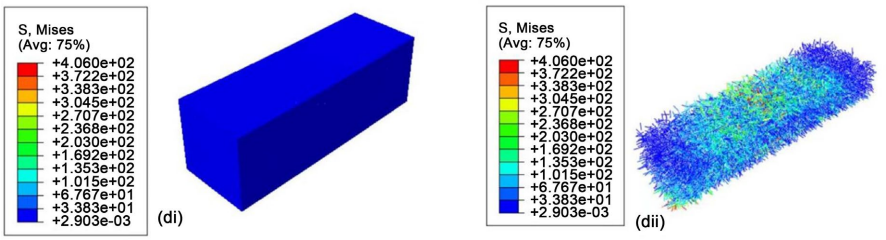

(d) 2.5% steel fiber volume ratio

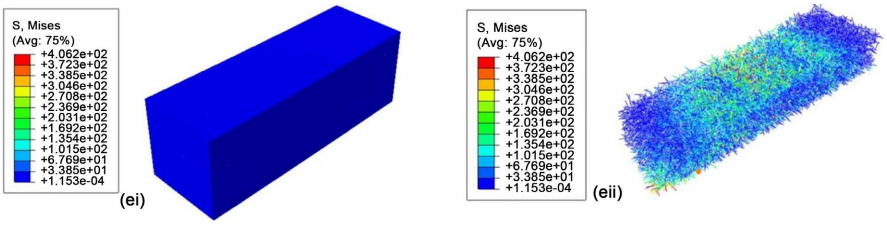

(e) 3% steel fiber volume ratio

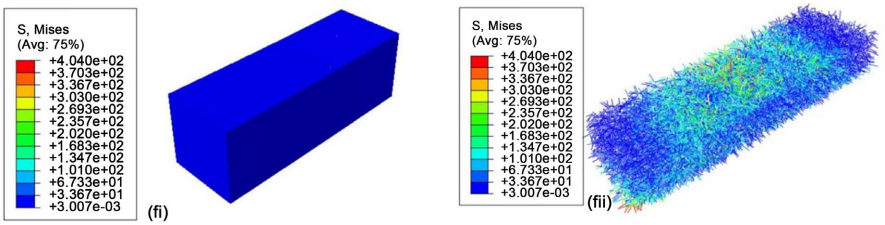

(f) 3.5% steel fiber volume ratio

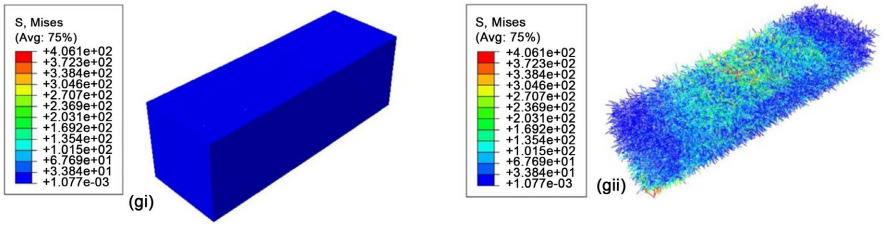

(g) 4% steel fiber volume ratio

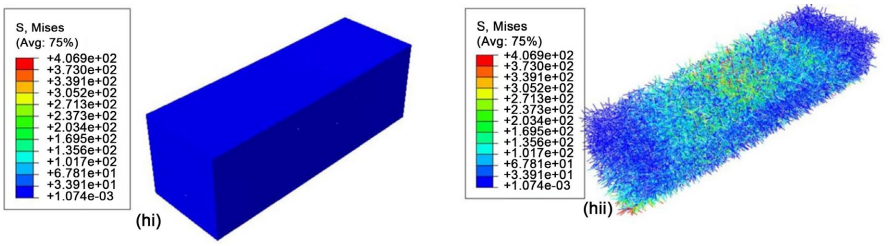

(h) 4.5% steel fiber volume ratio

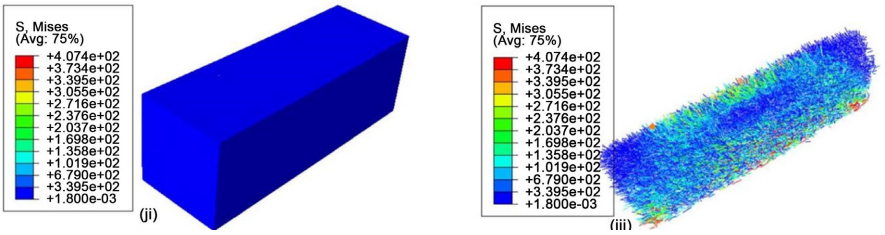

(i) 5% steel fiber volume ratio

Figure 11. Prism specimens and steel fibers after simulation test 1) exterior surface of the prism and 2) steel fibers.

3.3.3. Hybrid Fiber Trade-Offs

The hybrid recycled industrial and microfibers in concrete prisms reduced ductility under flexural loading. A ductility index ≥ 2 indicates high ductility, while values slightly below suggest semi-ductility; lower values denote brittleness, leading to sudden failure. Steel fibers typically enhance ductility, but the 2.5% hybrid mix showed the highest index (1.7145), with 3% and 3.5% mixes scoring lower (1.429 and 1.4628), confirming reduced ductility. The 3.5% specimen had the lowest flexural strength (11.8017 MPa) despite its high peak load, indicating that excess recycled fibers diminished flexural performance and stiffness. Spectral analysis (**Figure 12**) revealed failure at low-stress levels, with fibers absorbing less stress than the concrete matrix in previous tests, resulting in inadequate resistance to flexural stresses. **Table 6** shows calculated evaluations for hybrid fiber tests.

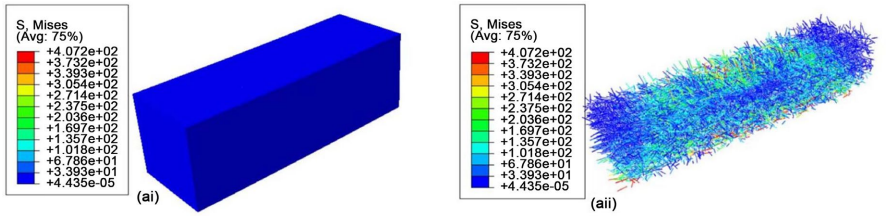

(a) 2.5% steel hybrid fiber volume ratio

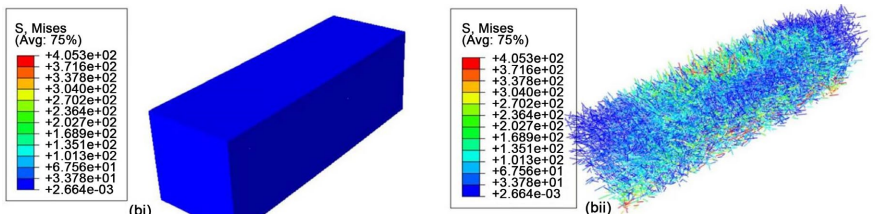

(b) 3% steel hybrid fiber volume ratio

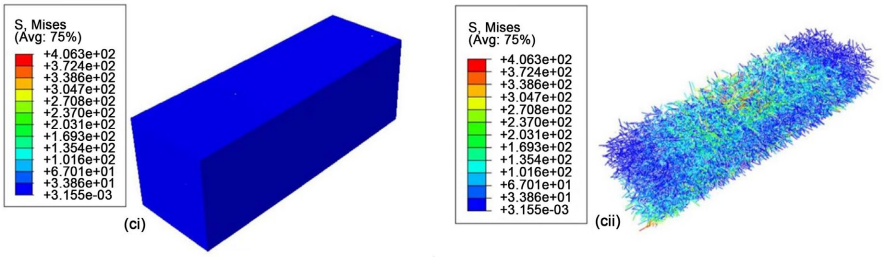

(c) 3.5% steel hybrid fiber volume ratio

Figure 12. Steel fibers after simulation test for concrete specimens containing industrially recycled steel fiber 1) prism's exterior surface and 2) steel fibers orientation.

3.4. Comparison between Laboratory Experimental Results with ABAQUS Simulation Results

The modulus of elasticity (E), representing the slope of the linear elastic region in the stress-strain curve, was determined between 0.3 and 0.5 of the peak stress to minimize the influence of early-stage micro cracking and plastic deformation, thereby providing a more reliable reflection of the material's elastic behavior [25]. Experimental results demonstrated a direct correlation between compressive strength and (E) at lower steel fiber volume ratio (Vf), The optimal E in laboratory tests occurred at fiber volume ratio (Vf) = 2.5%, with negligible variation below this threshold, suggesting a limit to fiber efficacy in enhancing elastic stiffness. Prior studies attributes this plateau effect to increased porosity from fiber clustering in (UHPFRC) [25]. ABAQUS simulations produced systematically higher E values, likely due to idealized material assumptions (e.g., perfect fiber-matrix bonding). While (E) was low at fiber volume ratio (Vf) = 1 − 1.5%, it peaked sharply at 3.5%, and became unstable beyond this point, with a notable dip at 4% before recovering at 5%. Although the highest simulated E occurred at fiber volume ratio (Vf) = 5%, the 3.5% mix seemed optimal due to its stability, whereas experiments identified 2.5% as the most effective. This divergence underscores the limitations of homogenized numerical models in capturing real-world complexities such as fiber dispersion and defect-induced softening, particularly at higher fiber volume ratio (Vf) where material heterogeneity dominates. The experimental plateau in E beyond = 2.5% and fiber volume ratio (Vf) = 3.5% for ABAQUS simulations further indicates a saturation point for fiber reinforcement in elastic deformation resistance, a critical insight for optimizing UHPFRC design. **Figure 13** shows the comparison of modulus of elasticity. Other studies reveals that modulus of elasticity increases with an increase in steel fiber volume (Vf) [41], however, modulus of elasticity reduces at 4% fiber volume [40]. This signifies that increase in steel fiber volume (Vf) up to 3.5% has a positive influence on the mechanical properties of concrete but fiber volume beyond that deteorates the UHPC mechanical performance due to agglomeration of fiber [4] leading to more pores and internal defects with unfavourably insufficient density of hardened UHPFRC and large void ratio [25].

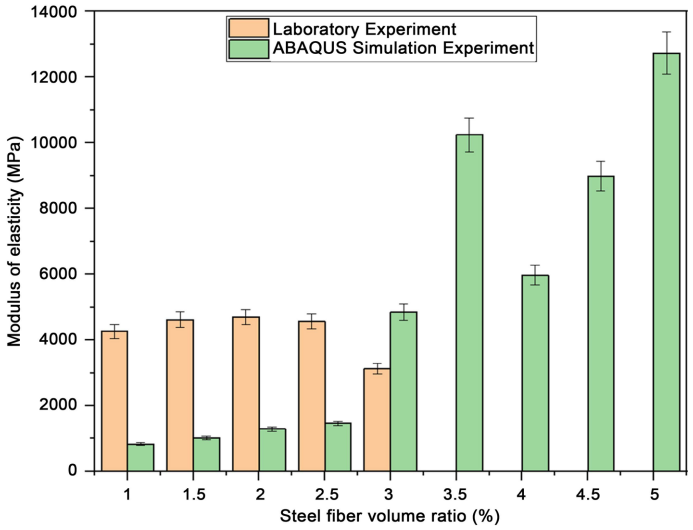

Figure 13. Comparison of modulus of elasticity.

The flexural behavior of steel fiber-reinforced concrete prisms was first investigated through laboratory experiments, revealing a direct correlation between fiber content and flexural strength. The minimum strength of 5.2 MPa was recorded at 1% steel fibers, while the maximum of 10.68 MPa was achieved at 3%. Beyond this threshold, a slight reduction in strength was observed, suggesting an optimal fiber reinforcement ratio for maximizing flexural capacity. Complementing these findings, ABAQUS simulations demonstrated a similar trend, with flexural strength increasing sharply between 2% and 2.5% before reaching an optimum of 13.405 MPa at 3%. Beyond this point, a marginal decline occurred, reinforcing the experimental conclusion that steel fibers exhibit peak effectiveness up to 3%. **Figure 14** compares the flexural strength from laboratory experiments and ABAQUS simulation results.

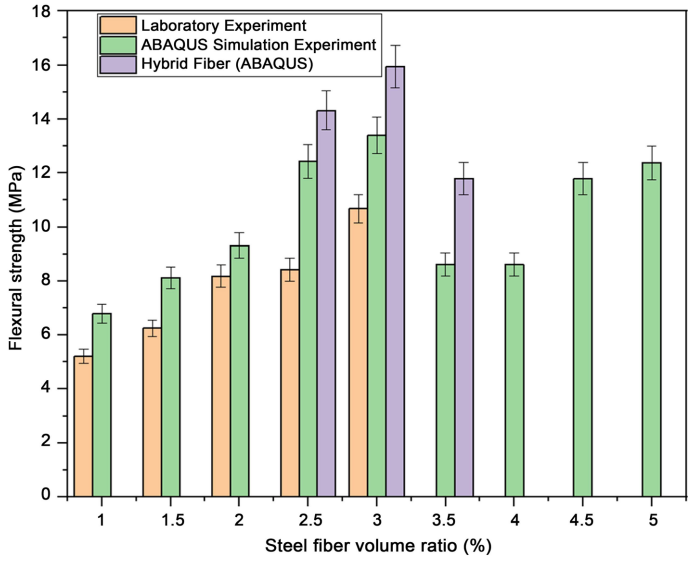

Figure 14. Comparison of flexural strength.

The simulations further highlighted load-bearing performance, with the minimum peak load at 55.44 kN (1%) and the maximum at 186.37 N (5%), confirming that incremental fiber volume ratio (Vf) enhances structural resistance. Additionally, ductility improved consistently with fiber content, mitigating brittle failure. However, post-peak stiffness diminished beyond 3.5%, indicating reduced fiber efficiency in the post-cracking phase. Both experimental and numerical analyses exhibited a linear load-deflection relationship in the elastic stage, while the softening phase in simulations showed increased deflection tolerance at higher fiber ratios, underscoring steel fibers' role in enhancing deformation capacity.

However, the introduction of a hybrid fiber mix (recycled industrial and microfibers) introduced trade-offs. The 3.5% hybrid specimen displayed the lowest flexural strength (11.80 MPa) despite achieving the highest peak load, suggesting compromised stiffness. Ductility was also affected, as the highest index (1.7145 at 2.5%) declined at higher ratios (1.429 at 3%, 1.4628 at 3.5%). This indicates that hybrid fibers, while improving load capacity, may not sustain ductility as effectively as pure steel fibers. Figure 15 shows the ductility performance, with hybrid fiber specimens exhibiting the lowest ductility index.

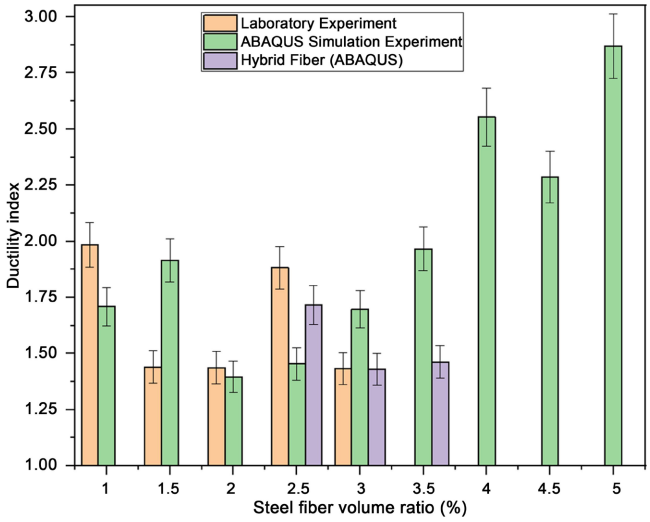

Figure 15. Comparison of ductility index.

These findings emphasize optimizing fiber content within the 2.5% - 3.5% range to balance strength, ductility, and post-cracking performance. A 3% steel fiber content emerged as the most effective for flexural enhancement, while hybrid mixes require further refinement to mitigate ductility reductions.

In laboratory experiments, UHPC prism specimens with higher steel fiber ratios demonstrated superior resistance to deformation, as reflected in their service stiffness—a key engineering parameter for pre-crack deformation resistance. The minimum service stiffness was 15.57 kN/mm at a 1% steel fiber volume ratio, while a 1.5% ratio doubled this value. At 2%, service stiffness peaked at 107.7 kN/mm, marking a 3.5-fold increase over the 1.5% ratio and representing the most effective enhancement. Further increments (2.5% to 3%) yielded diminishing re-

turns, improving stiffness by only 1.06 times.

ABAQUS simulations showed that service stiffness reached optimal stability at a 3.5% steel fiber ratio, beyond which performance became erratic. Figure 16 illustrates the relationship between service stiffness and fiber volume ratio.

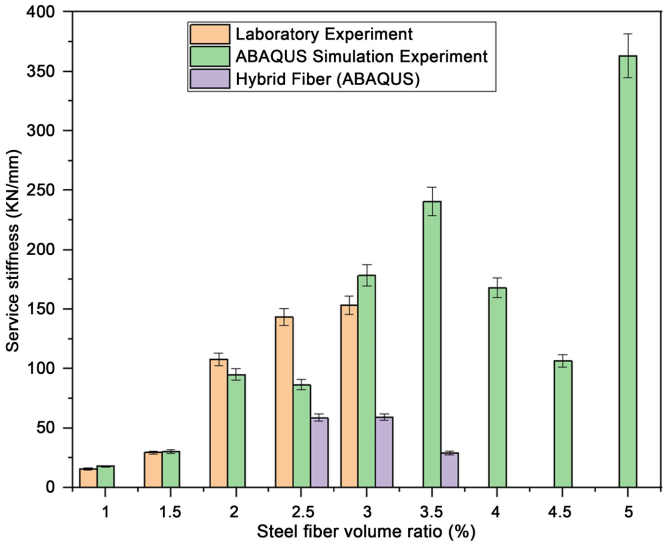

Figure 16. Comparison of service stiffness.

In lab tests, post-peak stiffness increased steadily with fiber content, peaking at 2.5%. In contrast, simulations and hybrid fiber specimens achieved optimum post-peak stiffness at 3.5%. However, hybrid mixes underperformed compared to pure micro steel fiber specimens, indicating the need for further research to optimize hybrid ratios (combining micro and recycled steel fibers) for improved post-peak behavior. Figure 17 compares post-peak stiffness across different steel fiber volume ratios.

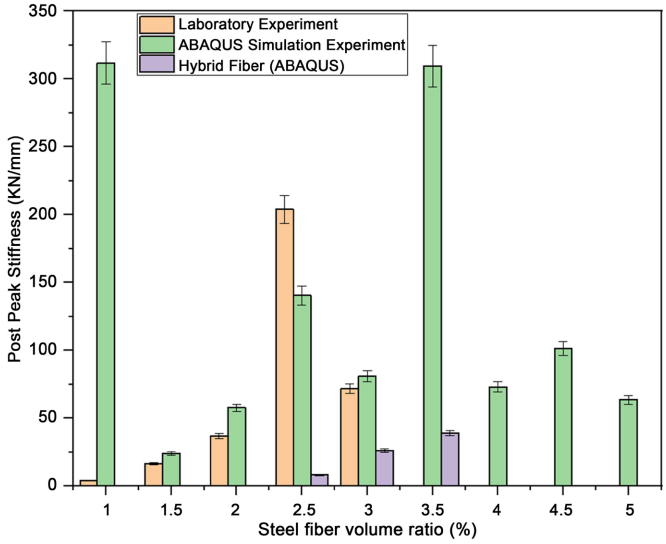

Figure 17. Comparison for Post peak stiffness.

A cutting-edge review study on fiber utilization in UHPC analyzed steel fiber performance data from a broad spectrum of 213 studies, concluding that the optimal steel fiber volume ratio should not exceed 3% [42]. This finding aligns with the evaluations presented in this paper, which identify an optimal steel fiber ratio between 3% and 3.5%, as illustrated in **Table 7**.

Table 7. Test specimens that had an effective optimum contribution to the compression and flexural strength parameters according to experimental results for laboratory experimental evaluations, ABAQUS simulations for micro steel fibers and ABAQUS simulation results for hybrid mix fibers programs 1 and 2.

Parameters of Test Results	Laboratory experimental evaluation	ABAQUS simulations for micro steel fibers	ABAQUS simulations for hybrid mix fiber
Peak state stress	3%	4.5%	---
Ultimate strain	3%	4.5%	---
Modulus of elasticity	2%	3.5%	---
Flexural strength	3%	3%	3%
Service stiffness	3%	3.5%	3%
Post peak stiffness	2.5%	3.5%	3.5%
Ductility index	2.5%	4%-5%	2.5%

4. Conclusion

This study investigated the influence of micro steel fibers and industrially recycled steel fibers on the mechanical properties of ultra-high-performance concrete (UHPC). The results demonstrated that steel fibers significantly enhance compressive strength, with ABAQUS simulations confirming their stress-absorbing capability. The optimal fiber content was identified as 3% - 3.5%, balancing cost and performance, as higher dosages primarily improved ductility and post-cracking resistance rather than strength. Hybrid fiber blends increased flexural strength but reduced ductility and stiffness, indicating a performance trade-off. A key limitation was the exclusive use of a 1:1 hybrid ratio, suggesting the need for future research on alternative blending proportions at fixed fiber volumes (e.g., 3% or 3.5%). The strong agreement between experimental and simulation results supports computational modelling as a reliable, cost-effective alternative to physical testing.

Further studies should explore diverse hybrid fiber ratios to optimize strength, sustainability, and cost efficiency, with recycled fibers offering an eco-friendly solution that aligns with circular economy principles in construction. Exploration on durability tests (carbonation resistance tests, chloride penetration tests and freeze-thaw resistance tests) will help in providing a clear understanding on of hybrid fiber mix design performance in harsh environmental conditions.

Conflicts of Interest

The authors declare no conflicts of interest regarding the publication of this paper.

References

[1] Abbas, S., Nehdi, M.L. and Saleem, M.A. (2016) Ultra-High Performance Concrete: Mechanical Performance, Durability, Sustainability and Implementation Challenges. *International Journal of Concrete Structures and Materials*, **10**, 271-295.

[2] Tayeh, B., Aadi, A., Hilal, N., *et al.* (2019) Properties of Ultra-High-Performance Fiber-Reinforced Concrete—A Review Paper.

[3] Yoo, D.-Y., Banthia, N. and Yoon, Y.-S. (2024) Recent Development of Innovative Steel Fibers for Ultra-High-Performance Concrete (UHPC): A Critical Review. *Cement and Concrete Composites*, **145**, Article 105359.

[4] Meng, W. and Khayat, K. (2018) Effect of Hybrid Fibers on Fresh, Mechanical Properties, and Autogenous Shrinkage of Cost Effective UHPC. *Journal of Materials in Civil Engineering*, **30**, Article 04018030.

[5] Sim, C., Tadros, M., Gee, D. and Asaad, M. (2020) Flexural Design of Precast, Prestressed Ultra-High-Performance Concrete Members. *Precast/Prestressed Concrete Institute Journal* (*PCI Journal*), **65**, 35-61.

[6] NPCA (2013) Ultra High Performance Concrete (UHPC), Guide to Manufacturing Architectural Precast UHPC Elements. National Precast Concrete Association.

[7] Zollo, R.F. (1997) Fiber-Reinforced Concrete: An Overview after 30 Years of Development. *Cement & Concrete Composites*, **19**, 107-122.

[8] Yan, X., Gao, Y., Luo, Y., Bi, Y. and Xie, Y. (2021) Effect of Different Steel Fiber Types on Mechanical Properties of Ultra-High Performance Concrete. *IOP Conference Series*: *Materials Science and Engineering*, **1167**, Article 012001.

[9] Yang, J., Chen, B., Su, J., Xu, G., Zhang, D. and Zhou, J. (2022) Effects of Fibers on the Mechanical Properties of UHPC: A Review. *Journal of Traffic and Transportation Engineering* (*English Edition*), **9**, 363-387. https://doi.org/10.1016/j.jtte.2022.05.001

[10] Rezakhani, R., Scott, D.A., Bousikhane, F., Pathirage, M., Moser, R.D., Green, B.H., *et al.* (2021) Influence of Steel Fiber Size, Shape, and Strength on the Quasi-Static Properties of Ultra-High Performance Concrete: Experimental Investigation and Numerical Modeling. *Construction and Building Materials*, **296**, Article 123532. https://doi.org/10.1016/j.conbuildmat.2021.123532

[11] Su, Y., Li, J., Wu, C., Wu, P. and Li, Z. (2016) Effects of Steel Fibres on Dynamic Strength of UHPC. *Construction and Building Materials*, **114**, 708-718. https://doi.org/10.1016/j.conbuildmat.2016.04.007

[12] Yoo, D., Soleimani-Dashtaki, S., Oh, T., Chun, B., Banthia, N., Lee, S., *et al.* (2024) Strain-Hardening Effect on the Flexural Behavior of Ultra-High-Performance Fiber-Reinforced Concrete Beams with Steel Rebars. *Developments in the Built Environment*, **17**, Article 100343. https://doi.org/10.1016/j.dibe.2024.100343

[13] Brandt, A.M. (2008) Fibre Reinforced Cement-Based (FRC) Composites after over 40 Years of Development in Building and Civil Engineering. *Composite Structures*, **86**, 3-9. https://doi.org/10.1016/j.compstruct.2008.03.006

[14] Huang, H., Gao, X., Li, L. and Wang, H. (2018) Improvement Effect of Steel Fiber Orientation Control on Mechanical Performance of UHPC. *Construction and Building Materials*, **188**, 709-721.

[15] Huang, H., Gao, X., Khayat, K.H. and Su, A. (2021) Influence of Fiber Alignment and

Length on Flexural Properties of UHPC. *Construction and Building Materials*, **290**, Article 122863. https://doi.org/10.1016/j.conbuildmat.2021.122863

[16] Mu, R., Chen, J., Chen, X., Diao, C., Wang, X. and Qing, L. (2023) Effect of the Orientation of Steel Fiber on the Strength of Ultra-High-Performance Concrete (UHPC). *Construction and Building Materials*, **406**, Article 133431. https://doi.org/10.1016/j.conbuildmat.2023.133431

[17] Spencer, R., Alwekar, S., Jo, E., *et al.* (2022) Fiber Orientation Evaluation in Reinforced Composites Using Digital Image Correlation and Thermal Excitation. *Composites Part B: Engineering*, **234**, Article 109713.

[18] Kang, S. and Kim, J. (2011) The Relation between Fiber Orientation and Tensile Behavior in an Ultra High Performance Fiber Reinforced Cementitious Composites (UHPFRCC). *Cement and Concrete Research*, **41**, 1001-1014. https://doi.org/10.1016/j.cemconres.2011.05.009

[19] Li, W., Zhao, Y., Zhang, Y., Xie, Z., Zhang, J., Huang, F., *et al.* (2024) Optimized Mix Design Method of Ultra-High Performance Concrete (UHPC) and Effect of High Steel Fiber Content: Mechanical Performance and Shrinkage Properties. *Journal of Building Engineering*, **97**, Article 110746. https://doi.org/10.1016/j.jobe.2024.110746

[20] Ren, G.M., Wu, H., Fang, Q. and Liu, J.Z. (2018) Effects of Steel Fiber Content and Type on Static Mechanical Properties of UHPCC. *Construction and Building Materials*, **163**, 826-839. https://doi.org/10.1016/j.conbuildmat.2017.12.184

[21] Wille, K., Naaman, A.E., El-Tawil, S. and Parra-Montesinos, G.J. (2011) Ultra-High Performance Concrete and Fiber Reinforced Concrete: Achieving Strength and Ductility without Heat Curing. *Materials and Structures*, **45**, 309-324. https://doi.org/10.1617/s11527-011-9767-0

[22] Ahmad, S., Rasul, M., Adekunle, S.K., *et al.* (2019) Mechanical Properties of Steel Fiber-Reinforced UHPC Mixtures Exposed to Elevated Temperature: Effects of Exposure Duration and Fiber Content. *Composites Part B: Engineering*, **168**, 291-301.

[23] Ridha, M.M.S. (2024) Combined Effect of Natural Fibre and Steel Fibre on the Thermal-Mechanical Properties of UHPC Subjected to High Temperature. *Cement and Concrete Research*, **180**, 107510. https://doi.org/10.1016/j.cemconres.2024.107510

[24] Li, M., Cheng, Y.H. and Wu, H. (2025) Effects of Steel Fiber Content and Type on Projectile Impacting Resistance of UHPC: Mesoscale Analysis. *International Journal of Impact Engineering*, **198**, Article 105228.

[25] Yang, J., Chen, B. and Nuti, C. (2021) Influence of Steel Fiber on Compressive Properties of Ultra-High Performance Fiber-Reinforced Concrete. *Construction and Building Materials*, **302**, Article 124104.

[26] Gao, D., Zhang, W., Tang, J. and Zhu, Z. (2024) Effect of Steel Fiber on the Compressive Performance and Microstructure of Ultra-High Performance Concrete at Elevated Temperatures. *Construction and Building Materials*, **435**, Article 136830. https://doi.org/10.1016/j.conbuildmat.2024.136830

[27] Abbas, S., Soliman, A.M. and Nehdi, M.L. (2015) Exploring Mechanical and Durability Properties of Ultra-High Performance Concrete Incorporating Various Steel Fiber Lengths and Dosages. *Construction and Building Materials*, **75**, 429-441.

[28] Yoo, D. and Yoon, Y. (2015) Structural Performance of Ultra-High-Performance Concrete Beams with Different Steel Fibers. *Engineering Structures*, **102**, 409-423. https://doi.org/10.1016/j.engstruct.2015.08.029

[29] Yoo, D.-Y., Kang, S.-T. and Yoon, Y.-S. (2016) Enhancing the Flexural Performance of Ultra-High-Performance Concrete Using Long Steel Fibers. *Composite Structures*,

147, 220-230.

[30] Bjegović, D., Baricevic, A., Lakusic, S., *et al.* (2014) Positive Interaction of Industrial and Recycled Steel Fibres in Fibre Reinforced Concrete. *Journal of Civil Engineering and Management*, **19**, S50-S60.

[31] Lee, J. and Fenves Gregory, L. (1998) Plastic-Damage Model for Cyclic Loading of Concrete Structures. *Journal of Engineering Mechanics*, **124**, 892-900.

[32] Ren, X. and Li, J. (2013) Multi-Scale Based Fracture and Damage Analysis of Steel Fiber Reinforced Concrete. *Engineering Failure Analysis*, **35**, 253-261.

[33] Toutlemonde, F., Kretz, T., Généreux, G., *et al.* (2018) Rougeau, French Standards for Ultra-High Performance Fiber-Reinforced Concrete (UHPFRC).

[34] AASHTO (2020) AASHTO LRFD Bridge Design Specifications. 9th Edition, American Association of State Highway and Transportation Officials (AASHTO).

[35] Park, R. (1989) Valuation of Ductility of Structures and Structural Assemblages from Laboratory Testing. *Bulletin of the New Zealand National Society for Earthquake Engineering*, **22**, 155-166.

[36] Huang, J., He, Z., Khan, M., Zheng, X. and Luo, Z. (2021) Flexural Behaviour and Evaluation of Ultra-High-Performance Fibre Reinforced Concrete Beams Cured at Room Temperature. *Scientific Reports*, **11**, Article 19069.

[37] El-Helou, R.G. and Graybeal, B.A. (2022) Flexural Behavior and Design of Ultrahigh-Performance Concrete Beams. *Journal of Structural Engineering*, **148**, Article 04022013. https://doi.org/10.1061/(asce)st.1943-541x.0003246

[38] Baran, E. and Arsava, T. (2012) Flexural Strength Design Criteria for Concrete Beams Reinforced with High-Strength Steel Strands. *Advances in Structural Engineering*, **15**, 1781-1792.

[39] Siva, C.R. and Pankaj, A. (2019) Flexural Behavior of Reinforced Concrete Beams with High Performance Fiber Reinforced Cementitious Composites. *Journal of Central South University*, **26**, 2609-2622. https://doi.org/10.1007/s11771-019-4198-0

[40] Yoo, D., Lee, J. and Yoon, Y. (2013) Effect of Fiber Content on Mechanical and Fracture Properties of Ultra High Performance Fiber Reinforced Cementitious Composites. *Composite Structures*, **106**, 742-753. https://doi.org/10.1016/j.compstruct.2013.07.033

[41] Ahmad, S., Hakeem, I. and Azad, A.K. (2015) Effect of Curing, Fibre Content and Exposures on Compressive Strength and Elasticity of UHPC. *Advances in Cement Research*, **27**, 233-239. https://doi.org/10.1680/adcr.13.00090

[42] Gong, J., Ma, Y., Fu, J., Hu, J., Ouyang, X., Zhang, Z., *et al.* (2022) Utilization of Fibers in Ultra-High Performance Concrete: A Review. *Composites Part B: Engineering*, **241**, Article 109995. https://doi.org/10.1016/j.compositesb.2022.109995